CLASSIFICATION OF FINGERPRINTS USING SINGULAR POINTS AND THEIR PRINCIPAL AXES

C. Klimanee and D.T. Nguyen

School of Engineering – University of Tasmania
GPO Box 252-65 Hobart, Australia
d.t.nguyen@utas.edu.au

ABSTRACT

This paper proposes a rule-based algorithm for classification of a fingerprint into one of six well-known classes: plain arch, tented arch, right loop, left loop, whorl and twin loop. The rules are formed using the relative locations and types of singular points and the relative directions of their associated principal axes. The reliable and fast classification algorithm is made possible by a simple but effective combination of ridge *flow-code* technique and *orientation variance* calculation in the determination of singular points and principal axes. The Poincaré indices of these singular points are used to determine their type: ordinary, delta, core or double-core. For a small test sample of 157 fingerprints available to the authors, the correct classification rate is better than 90%.

1. INTRODUCTION

In most practical automatic fingerprint identification systems, it is necessary to reduce the extent of search of a database for the best-matched fingerprint. This can be achieved by a two-stage approach: a classification of the given fingerprint into one of the classes based on its *global* structure, followed by a search of the sub-database consisting of fingerprints of that particular class only. A fingerprint is uniquely identified by the distribution of its *local* structures such as ridge endings and ridge bifurcations known as *minutiae*. The well-known *Henry*'s classification scheme divides a fingerprint structure into three major classes or patterns: *Arch*, *Loop* and *Whorl*. Most people have loops but only a few have arches on their fingerprints. Researchers usually detail these three classes further into six or more subclasses or types based on finer differences within each class. In Figure 1 we distinguish six classes of fingerprints commonly found in practice: Plain Arch, Tented Arch, Right Loop, Left Loop, Double (or twin) Loop and Whorl (Plain or Accidental).

The global structures of a fingerprint such as *singular points* and their associated *principal axes* of the dominant ridge flow directions radiated from the singular points characterise fingerprint classes very reliably. In this paper we now propose a new technique for the determination of both singular points and their associated principal axes. We then present an algorithm for fingerprint classification using these global structures. Our classification algorithm is more accurate than those proposed in [2] and [3] owing to three factors: the higher resolution of the estimated orientation field, the more accurate location of singular points and the new concept of their associated principal axes. Our more quantitative approach effectively eliminates the frequent confusion between an arch and a tented-arch encountered in [3]. The automatic recognition between a whorl and a twin loop proposes a significant challenge to researchers. In [3] theses two classes are combined into one and the challenge is not addressed.

2. HIGH RESOLUTION ORIENTATION FIELD ESTIMATION

Most current ridge orientation estimation techniques are based on some variants of mean square optimisation [1], and for this to be reliable, the estimation window or block size has to be wide enough for the technique to have immunity to noise. The doubling of the gradient vectors due to the squaring process overcomes the bi-directional (or 180^0) ambiguity of the ridge orientation. In this paper, we adopt the mean square derivation in [1] by squaring the gradient vectors, i.e. squaring the magnitude and doubling the angle, before taking the mean over the whole block. Most authors use a block size of 8x8 or even 16x16 pixels for ridge orientation estimation. We propose to double the *gradient* resolution to 4x4 pixels by first estimating the ridge gradients on a *quincunx* grid. This is achieved by estimating two overlapping gradient fields both using the usual 8x8 pixels estimation block size on a rectangular grid, but one is shifted *diagonally* from the other field by $4\sqrt{2}$ pixels.

0-7803-8554-3/04/$20.00 ©2004 IEEE.

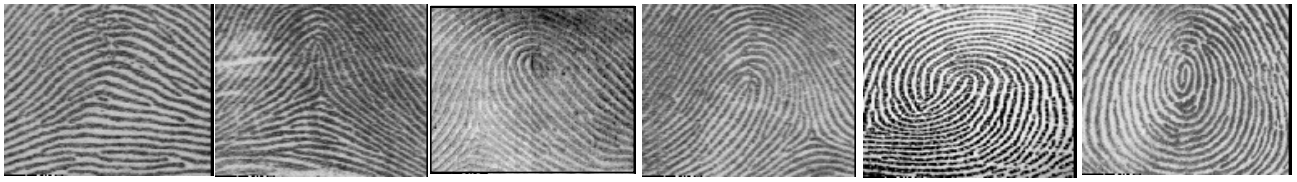

Plain arch Tented arch Right loop Left loop Twin loop Whorl

Figure 1: Six classes of fingerprint commonly found in practice

The two gradient fields are then merged together into a single quincunx field of 4x4 pixels resolution. The computation requirement is thus only doubled. To complete the final 4x4 pixels rectangular gradient field it is necessary to interpolate the gradients at the pixels halfway between the pixels on the quincunx grid at which the gradients are already known. Finally, the gradient angles $-90^0 \le \phi(u,v) < 90^0$ are calculated from their horizontal and vertical components. The ridge orientation $0^0 \le \theta(u,v) < 180^0$ is obtained simply by adding 90^0 to $\phi(u,v)$.

3. THE RIDGE FLOW CODE

To quickly locate the regions containing singular points, we propose to quantise the ridge orientation into *six* codes. Thus each 4x4-pixel block is assigned a *ridge flow code* and a fingerprint is coded into a *ridge flow map* as illustrated in Figure 2b for a tented-arch fingerprint. *Singular regions* are regions in which ridge orientation changes sharply and in a complex manner and are found by locating those blocks in the ridge flow map where *all six* codes exist or converge. *Singular points* are expected to be found in these singular regions. Global patterns of fingerprints are characterised by regions or segments of relatively uniform ridge orientation, i.e. having the same flow code. In this paper, singular region is defined as the cluster of connected 7x7 blocks all having the maximum of six codes. The boundaries of the ridge flow regions can simply be determined from trajectories of the 2-code blocks. Figure 2 shows the result for a tented-arch fingerprint. In 2(c) the two singular regions are clearly shown in white and the flow region boundaries are shown by grey lines.

4. DETERMINATION OF SINGULAR POINTS

Once a singular region on a fingerprint has been determined, we *only* search this small region for the corresponding singular point. We make use of the *local* variance of orientation to determine the locations of singular points as where the variance is maximum. The local variance of the orientation field at a block (x,y) is calculated over a region of 3x3 blocks centred on (x,y). Let $\nabla\theta_{p,q}(x,y)$ be the difference in orientation between the block(x,y) and its adjacent block(x+p,y+q), then to take care of the 180^0 ambiguity in θ we must have

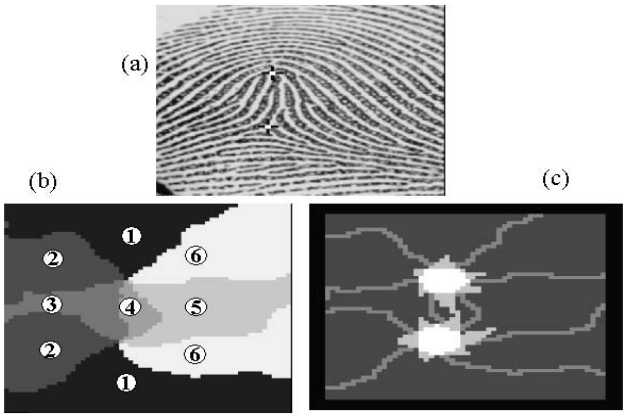

Figure 2: (a) Tented Arch fingerprint, (b) its ridge flow map, and (c) its singular regions of 6 codes (in white) and flow region boundaries of 2 codes (in grey lines).

$$\nabla\theta_{pq}(x,y) = \min\left\{\begin{matrix}\left|\theta(x,y) - \theta(x+p, y+q)\right|, \\ 180^0 - \left|\theta(x,y) - \theta(x+p, y+q)\right|\end{matrix}\right\}, \quad p,q = -1,0,+1 \tag{1}$$

Researchers have identified four common types of singular points [3]: *Ordinary*, *Delta*, *Core* and *Double-Core*, named after their visual shape. Thus a plain arch has neither cores nor deltas while a tented arch has a delta and a core. A loop also has a core plus a neighbouring delta. As in [2,3], we use the Poincaré index to identify the type of a singular point.

When the point (x,y) moves once around a closed contour C in a counter-clockwise direction (conventionally positive) the Poincaré index is defined in discrete form as

$$I(C) = \frac{1}{2\pi}\sum_{i=1}^{N} \nabla\theta_i \tag{2}$$

When applying the Poincaré index to the ridges of a fingerprint, because the line function has 180^0 ambiguity, we must choose the *smaller* of the two complementary angles for the difference between the two orientations. If $I(C)$ = 0, -1/2, +1/2 or 1, the contour C contains an *ordinary* point, a delta, a core or a double core, respectively, in its interior.

In [2,3], singular points are found by computing the Poincaré index of every orientation estimation block. The accuracy of the locations of the singular points is therefore limited to within the estimation block size of 16x16 pixels in [2] and 8x8 pixels in [3] compared to 4x4 pixels in this paper. Our approach in this paper achieves a higher resolution for ridge orientation and a much simpler algorithm, hence much faster, singular point detection. This is because we have to compute the Poincaré index only for singular points to determine whether they are deltas, cores or ordinaries. With the high accuracy produced by the proposed algorithm for the location of singular points, the Poincaré index almost always gives the correct type of singular points. In this paper, we choose the summing contour *C* in (2) as the 16 connected blocks in the *outer* of the 5x5-block neighbourhood centred at the singular block. We have found that if rotation is moderate, say less than 20^0, the proposed technique is found to be reasonably scale and rotation invariant for all fingerprints in Figure 1.

5. DETERMINATION OF PRINCIPAL AXES

Principal axes associated with a singular point are defined as the axes radiated from the point and having the dominant directions of the ridge flow near the singular point. The directional relationship between the principal axes and the axes joining the singular points, i.e. core-to-core and core-to-delta axes, effectively characterises the global structure of the fingerprint. Principal axes are therefore useful for distinguishing classes having the same number and type of singular points.

The topology of a loop, just outside the singular point, is characterised by the dominance of the almost parallel ridges in its 'tail', and by the almost semicircular ridges around the core at its 'head'. For a tented arch, the tail actually 'flares' out from the core and we can expect to have two dominant orientations. A loop that has a 'fat' head may have one more dominant ridge orientations apart from that of its tail, that has to be suppressed. We achieve this by using an *orientation mask* which excludes the inner region around a singular point and suppresses *non-radial* orientations. The radial orientations are calculated from the block centres to the singular point. With the above observations, we propose the following algorithm:

Step 1: Consider an 'annular' region of size 15x15 blocks centred on a core and the excluded centre is 7x7 blocks.
Step 2: Subtract the orientation field in the annular region from that of a 15x15-block orientation mask.
Step 3: Threshold the difference orientation field by 45^0 and retain only those blocks with difference orientation smaller than the threshold.
Step 4: Plot the histogram of the orientations θ of the blocks surviving from the thresholding in Step 3, $0<\theta\leq 180^0$ using a bin-size of 10^0.
Step 5: Determine the dominant orientations (θ_{pi}, f_{pi}), i.e. the histogram peaks.
Step 6: If two adjacent peaks are separated from each other by only one bin-size, group them into one group keeping the middle component.
Step 7: If the adjacent component to a peak is stronger than *half* the strength of the peak, retain the component. This step together with Step 6 results in peaks θ_{pi} of width w_i, where $1\leq w_i \leq 5$ bin-sizes.
Step 8: Calculate the probability that orientation belongs to peak at θ_{pi}, which is

$$\Pr(\theta_{pi}) = \frac{1}{N}\sum_{k\in w_i} f_k \qquad (3)$$

It is important that w_i is kept the same for all peaks, i.e. same number of components is summed up in (3).
Step 9: Retain only the peak with the highest probability and those with a probability equal or better than 30% of the highest probability. The surviving peaks give the estimate of the dominant orientations in the loop's tail.

Figure 5 gives the estimated principal axes of a tented arch and a right loop. The chosen loop is rather 'fat' having pronounced orientation around its head and hence is prone to having a second dominant orientation axis. The proposed mask in Figure 4 has successfully eliminated that orientation from its histogram.

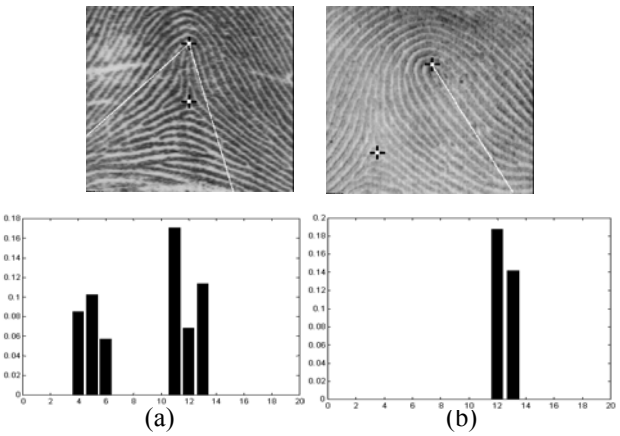

(a) (b)

Figure 5: Estimated principal axes of (a) a tented arch, and (b) a right loop

6. CLASSIFICATION ALGORITHM

Our fingerprint classification algorithm uses a ruled-based approach based on the number and type of singular points and the relative direction of their associated principal axes. It therefore depends a great deal on the accuracy of the location of the detected singular points and the

direction of the corresponding principal axes. A wrong location can give a zero Poincaré index, hence missing out the singular point. An inaccurate location of a core can also give rise to a second dominant axis, thus confusing a loop with a tented-arch. The algorithm distinguishes a whorl from a twin loop using the relative direction of the two principal axes with respect to the core-to-core axis. The proposed algorithm for fingerprint classification is summarised in Figure 6.

7. RESULT AND CONCLUSION

We have successfully presented a simple technique for the detection of singular points and their associated principal axes on a fingerprint. The accurate detection of these two characteristic global structures of fingerprints has allowed us to propose an improved classification algorithm compared to current ruled-based techniques. For a small database of only 157 fingerprints being available to us, the classification result is recorded in Table 3 with an overall correct classification rate of 9.33%. An outcome is rejected when singular points are not detected in core-delta pairs. The separation of a whorl from a twin loop presents by far the most challenging task. Previous researchers, e.g. [3], did not tackle this difficulty but combined whorl and twin loop into a single class.

Table 3: Result of Classification

True class / Assigned	Plain arch (19)	Tented arch (11)	Whorl (34)	Left loop (47)	Right loop (34)	**Twin loop** (12)
Plain arch	17	1	0	1	1	0
Tented arch	1	8	0	0	1	0
Whorl	0	0	29	0	0	2
Left loop	0	0	0	43	0	0
Right loop	0	1	0	0	30	0
Double loop	0	0	5	0	0	10
Reject	1	1	0	3	2	0

REFERENCES

[1] A.M. Bazen and S.H. Gerez, "Directional Field Computation for Fingerprints Based on the Principal Component Analysis of Local Gradients," *Proceedings ProRISC 2000 Workshop on Circuits, Systems and Signal Processing,* Veldhoven, The Netherlands, Nov. 2000.

[2] M. Kawagoe and A. Tojo, "Fingerprint Pattern Classification," *Pattern Recognition*, Vol. 17, No. 3, pp. 295-303, 1984.

[3] K. Karu and A.K. Jain, "Fingerprint Classification," *Pattern Recognition*, Vol. 29, No. 3, pp. 389-404, 1996.

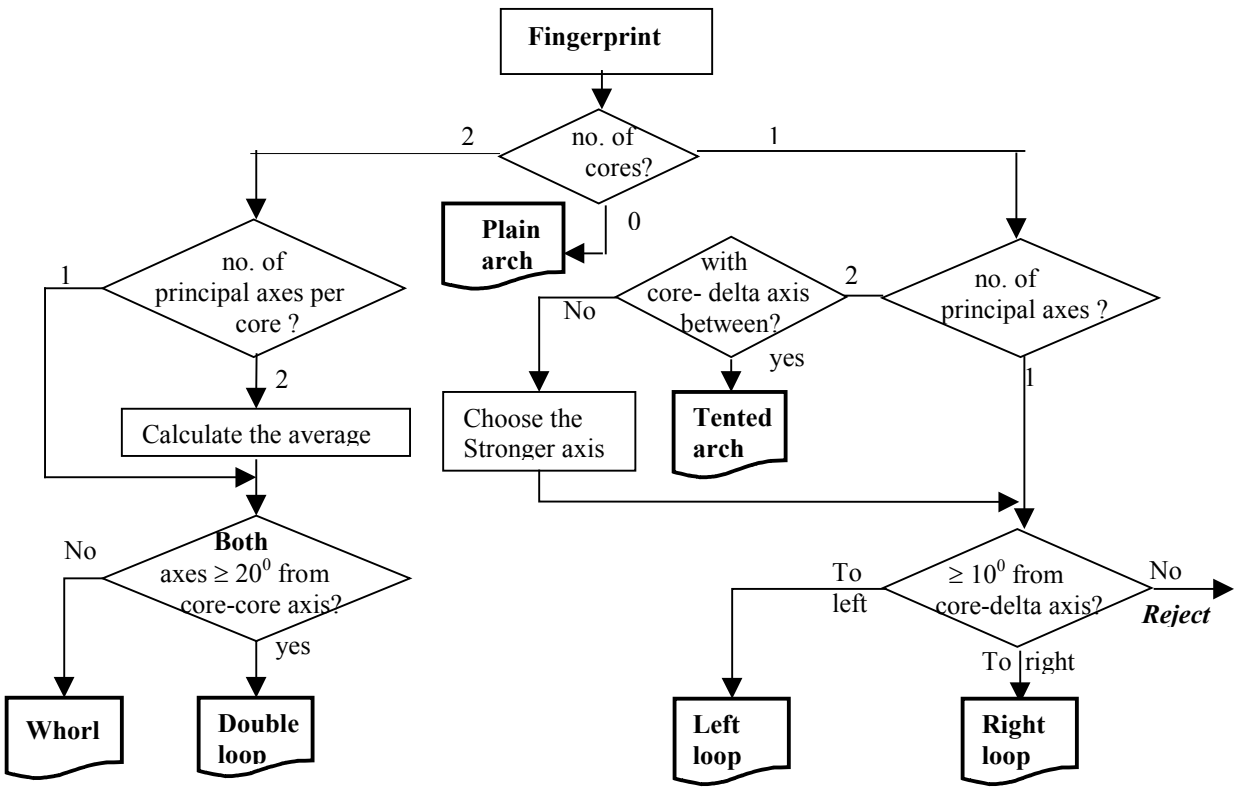

Figure 6: Proposed fingerprint classification algorithm using singular points and their principal axes